The Range and Straggling of Protons between 35 and 120 Mev*

N. BLOEMBERGEN† AND P. J. VAN HEERDEN
Nuclear Laboratory, Harvard University, Cambridge, Massachusetts
(Received March 12, 1951)

The range of protons in aluminum, copper, and lead has been determined with a photographic method, using the internal beam of the 95-in. synchrocyclotron of Harvard University. The method allows the simultaneous determination of the range, straggling, and the energy distribution of the protons in the internal beam. The latter was shown to have a half-width of 12 Mev. The experimental results for the range show slight, but significant deviations from tabulated values. Results for the straggling agree well with theory, if the effect of multiple scattering in the absorber is taken into account.

I. INTRODUCTION

THE energy loss, and, therefore, the range of heavy charged particles in matter, is almost completely determined by ionization and excitation of atoms. For energies below 10 Mev, there is abundant experimental material for the range of charged particles, and Bethe's formula[1] for the energy loss per unit path,

$$-dE/dx=(4\pi NZz^2e^4/mv^2)[\log(2mv^2/I)-\log(1-\beta^2)-\beta^2], \quad (1)$$

describes the results well. Calculations based on Eq. (1) have been extended to higher energies,[2,3] and ranges in many substances have been tabulated up to 10,000 Mev. These tables are often used in the determination of the energy of a particle by means of its range, but the only experimental check, reported recently[4] during the course of this work, is for protons of 345 Mev. It is true that no large deviations from the tabulated values are to be expected, since Bethe's formula is well fitted to the experimental data below 10 Mev and the underlying assumptions are even better fulfilled at higher energies, as long as energy losses by meson production and radiation can be neglected. But the mean ionization potential, I, has not been calculated precisely by the theory, and usually a rather arbitrary assumption like the approximate relation[2] $I=11.5Z$ is made. The quantity I should be determined from experiment. Small differences of our observed ranges from the tabulated values[2] lead to different values for I. These results will be given in Sec. III after the description of a new method by which they have been obtained.

In a final section the energy distribution of the protons in the internal beam of the synchrocyclotron will be discussed. It is an important factor in the interpretation of experiments with the internal beam and should always be taken into account.

II. EXPERIMENTAL METHOD

The beam hitting a target in a synchrocyclotron is not monoenergetic. The energy of the protons is defined in the following way. The particles are scattered into a narrow forward cone by coulomb forces in a thin tungsten target which is placed inside the dee. The protons are refocused by the magnetic field of the cyclotron according to their momentum in the horizontal plane. There is no focusing for the small vertical component of the motion. The protons which are scattered slightly downward hit the plateholder assembly located three inches below the medium plane of the cyclotron on a radius about 180° from the scatterer. A sketch of the situation is given in Fig. 1.

For each setting of the target, an interval of about 20 Mev can be covered at the plate, where the protons are selected according to energy. Both target and plateholder could be moved inward to obtain data at lower energies. The target was set at about 40 in., 35 in., 30 in., and 25 in., and each time the photographic plates covered a distance of 10 in. inward from the target radius. The position of the target and the plate was measured with a precision of 0.5 mm.

The magnetic field was calibrated along several radii to one part in ten thousand with the magnetic resonance of the Li^7 nuclei.[5] It appeared that the field values were reproducible to within 0.05 percent by adjusting the regulated magnet current to a standard value. Thus, the field was not recalibrated during each

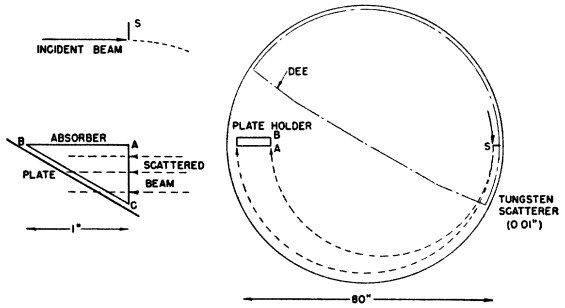

FIG. 1. Schematic diagram showing the positions of target, absorber, and photographic plate inside the tank of the cyclotron.

* Assisted by the joint program of the ONR and AEC.
† Society of Fellows.
[1] M. S. Livingston and H. A. Bethe, Revs. Modern Phys. **9**, 261 (1937).
[2] Aron, Hoffman, and Williams, Report AECU-663, UCRL-121 (1949).
[3] J. H. Smith, Phys. Rev. **71**, 32 (1947).
[4] C. J. Bakker and E. Segrè, Phys. Rev. **81**, 489 (1951).
[5] We are indebted to Mr. G. D. Watkins and Mr. U. E. Kruse for carrying out this calibration.

run. The energy can then be calculated from the Hr values with an accuracy of 0.2 percent at 40 in. and 0.3 percent at 25 in.

The range was determined by means of a tapered absorber which the protons had to traverse before they would hit the photographic emulsion of the Kodak commercial film. The intensity of the internally scattered beam would produce a convenient density after an exposure of a few seconds. Once the direction of the incoming protons was checked with a nuclear track plate, all data were taken with the unsensitive commercial film which was clamped between the plateholder and the absorber. The film could easily be changed by pulling the plateholder assembly out of the tank through a vacuum lock.

The absorbers were 10 in. long and had a triangular cross section with angles of 30° and 60°. The protons would enter the absorber perpendicular to the narrowest edge, which is about 0.5 in. high. The absorbers were made from electrolytic aluminum (measured density: 2.701 g/cm³), electrolytic copper (8.857 g/cm³), and chemically pure lead (11.32 g/cm³). The position of the absorber edge was marked on the film with a light source. In the case of lead, which had no sufficiently sharp edges, light marks were obtained through small drilled holes. After exposure and processing, the plates would show an appearance such as is schematically represented in Fig. 2. The r-direction represents the direction of increasing radius, thus increasing energy, and the y-direction increasing thickness of the absorber. There is a rather sharp slanting edge above which the plate is blank. No protons are able to traverse the absorber there.

The photographic density D was measured along lines in the y-direction for various values of r. A typical microphotometer curve is given in Fig. 3. From the density the number of protons, N, hitting a unit area of the plate can be calculated with the formula,

$$D=Ga[1-\exp(-Na)], \qquad (2)$$

where G is the number of grains per cm² emulsion with an average cross section a; furthermore, $D_M=Ga$ is the maximum attainable density.[6] The assumption underlying Eq. (2) is that every grain traversed by a proton is made developable. This is not true for fast protons which produce a smaller density. But the registrogram in Fig. 3 shows that the density is nearly constant over a considerable distance near the end of the range, so that there formula (2) can be applied. Nuclear track plates are not as good in this respect. The smaller grains in these plates cause the density to decrease more rapidly, as the proton energy is increased. Since our experimental density was always smaller than unity ($D/D_M<\frac{1}{5}$), the approximate relation that N is proportional to D was used. The relative error in N is smaller than 10 percent. In this way an integral range curve can be obtained from Fig. 3. Examples are shown in Figs. 4 and 5. The distance from the absorber edge to the point where the number of protons has dropped to 50 percent multiplied by the cosine of the absorber angle gives the value for the mean range. The cosine was checked at many points in the absorber with a traveling microscope to eliminate machining inaccuracies. The uncertainty in the mean range is estimated at less than 0.003 cm.

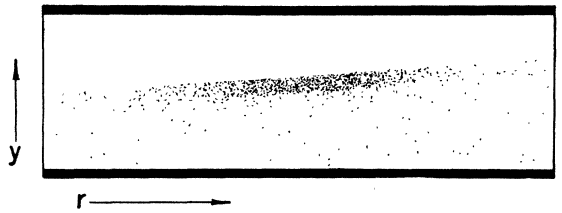

FIG. 2. Facsimile drawing of a photographic plate used in the measurements. The black horizontal lines at the top and bottom are the light marks, indicating the edge of the absorber. The slanting line indicates where the protons reach the end of their range. For further explanation see text.

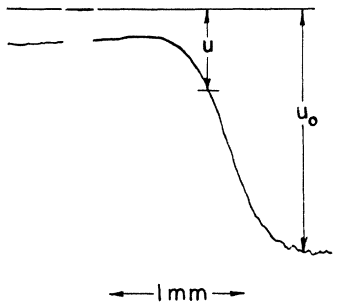

FIG. 3. Photometer curve of a plate along a line of constant r. The deflection u_0 corresponds to the blank plate; the deflection u is somewhere in the straggling part of the range. The photographic density is defined as $D=^{10}\log(u_0/u)$. The edges of the absorber fall far outside the diagram, which contains only a small portion in the y-direction across the slanting line of the plate in Fig. 2.

The straggling parameter s is simultaneously obtained, as indicated in Figs. 4 and 5. At lower energies (below 60 Mev), the straggling is enhanced by imperfect focusing. The focusing condition—at $\pi(1-n)^{-\frac{1}{2}}$ radians from the target—is not critical, since the protons emerge in a narrow cone with an aperture of about 1° from the thin scatterer. At 40 in. the plate was exactly in focus at 185° from the scatterer. Unfortunately, the geometry of the tank made it impossible to align plate and target at 180° for the smallest radii. In this case the plate was actually 20° out of focus. This caused an energy spread of about 0.6 percent and an apparent increase in the straggling of 50 percent. Straggling data below 60 Mev have, therefore, been omitted.

Corrections from not perfect normal incidence of the protons on the absorber and from the small contribution of the vertical component of the motion to the

[6] H. Yagoda, *Radioactive Measurement with Nuclear Emulsions* (John Wiley and Sons, Inc., New York, 1949), p. 22.

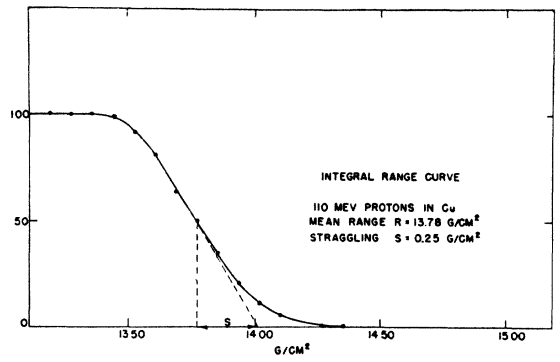

FIG. 4. Integral range curve for 110-Mev protons.

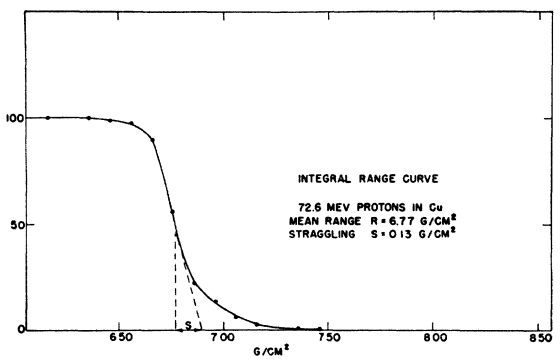

FIG. 5. Integral range curve for 75-Mev protons.

energy are smaller than 0.1 percent. About 10 percent of the protons are scattered inelastically or absorbed in nuclear reactions. But the effect of these processes on the range is negligible, as is also the effect of the curvature of the path through the absorber in the magnetic field.

The range can also be obtained from experiments with flat absorbers. Only protons with an energy sufficiently large to penetrate the absorber will reach the film. At smaller radii the film will be blank. The film is photometered in the r-direction, and a value for the energy with a mean range equal to the thickness of the absorber can be obtained. The photometer curve has to be corrected for the radial distribution in the number of protons (compare Sec. IV).

Strictly speaking, the curves obtained by the first method should be corrected for the vertical distribution in the number of protons. Over the small region of the absorber of interest in the experiments, this distribution is practically constant.

TABLE I. Range-energy relation for protons in copper.

Proton energy (Mev)	Theoretical range (grams/cm²)	Experimental correction (%) Run I	Run II	Run III	Flat abs.
113.7	14.79	+0.5	+0.5	+0.6	
111.3	14.24	+1.0	+0.8	+1.0	
108.3	13.58	+0.6	+0.7	+1.0	
102.1	12.26	+1.7	+1.8	+2.7	
99.8	11.78	+1.2	+0.7	+1.9	
96.2	11.19	0.0	+0.2	+0.5	
		+0.9±0.5	+0.7±0.2	+1.3±0.6	
89.8	9.79	+1.4	+1.6	+1.5	+1.0
86.9	9.24	+1.9	+1.5	+2.4	
84.0	8.71	+1.2	+1.5	+1.4	+1.3
79.1	7.84	+2.1	+1.6	+2.6	
76.1	7.32	+2.1	+2.6	+2.4	
73.0	6.81	+1.0	+1.7	+1.1	
		+1.6±0.4	+1.8±0.3	+1.9±0.6	+1.2
65.2	5.55				+2.2
					+1.2
55.7	4.23				+0.5
44.0	2.79				+1.2
					+1.3±0.4

III. RESULTS

The experimental results for the mean range in copper are listed in Table I. It is seen that there is a small but significant difference from the theoretical values obtained by interpolation in the tables of Aron, Hoffman, and Williams.[2] The experimental range is about 1 percent larger at the higher energies, and 1.5 percent at the lower. The mean of the absolute deviations has been listed. It is believed that the deviations from the mean are due to errors in the plateholder setting and in the measurement of absorber thickness. The deviations are in agreement with the estimated errors in the range and energy determination. The error could undoubtedly be reduced by a factor of 3 by a more painstaking definition of the geometry.

The data for aluminum are shown in Table II. The theoretical values are taken from Smith.[3] Again a

TABLE II. Range-energy relation for protons in aluminum.

Proton energy (Mev)	Theoretical range (grams/cm²)	Experimental correction (percent)
75.84	6.057	+0.1
75.70	6.041	+1.4
73.05	5.660	+0.7
72.94	5.657	+1.8
66.10	4.750	+0.5
65.78	4.711	+0.7
62.10	4.248	+0.5
61.79	4.205	+1.0
56.96	3.650	+1.2
56.68	3.626	+1.4
		+0.9±0.4
52.33	3.136	+1.4
52.08	3.106	+2.4
47.67	2.646	−0.3
		−1.1
44.86	2.372	+0.9
		+1.1
42.57	2.153	+2.5
		+1.1
39.66	1.907	+1.4
		+0.3
37.16	1.700	+3.7
		+2.4
34.96	1.511	+2.9
		+1.3
		+1.4±1.0

TABLE III. Range-energy relation for protons in lead.

Proton energy (Mev)	Theoretical range (grams/cm²)	Experimental correction (percent) Run I	Run II	Flat abs.
114.1	20.83	−1.0	−0.3	
106.6	18.54	−1.4	−1.4	
104.1	17.81	−1.5	−1.1	
95.3	15.30	−1.0	−1.0	
89.1	13.55	−0.7	0.0	
82.4	11.93	−1.1	−0.8	
78.9	11.12	−1.1	−0.9	−1.4
72.1	9.47	−0.5	−1.0	
62.5	7.42			−0.1
		−1.0±0.3	−0.9±0.4	−0.8±0.7

difference of 1 percent to 1.5 percent is observed. Finally, Table III shows the results for lead. Here the range is 1 percent smaller than the tabulated value.

The differences must be attributed to the average ionization potential. The value of this quantity derived from experiment and the relative mass stopping power at 75 Mev, with copper taken as reference, are given in Table IV. The ratio of the mass stopping powers for Cu and Pb agrees well with the value of Bakker and Segrè[4] at 300 Mev, but there is a discrepancy for the ratio of Al and Cu outside the limits of error of the two experiments. We think our value 1.221 to have a possible error of 1 percent, while Bakker and Segrè give 1.143 to be correct within 2 percent.

Our range measurements for Al, however, yield a value for I_{exp} in fair agreement with Wilson's measurement.[7] He derives for the mean ionization potential of Al 150±5, while we get 159±5.

Consequently, our values of I_{exp} at 100 Mev for Cu and Pb are substantially larger than those at 300 Mev reported by Bakker and Segrè.

The last column in Table IV gives the values I_{corr}, if the effect of multiple scattering of protons traversing the absorber is taken into account. Since the particles will not follow a straight line through the absorber, the real range will be larger than the measured one.

The mean square deviation in angle from the normal direction at a distance (R_0-x) in the absorber is given by[8-10]

$$\langle\vartheta^2(x)\rangle_{\text{Av}}=\int_{-R_0}^{-x}4\pi Ne^4Z^2G(pv)^{-2}dx^1, \tag{3}$$

where N is the number of nuclei per cc with charge Z, p and v the momentum and the velocity of the proton, and G is a numerical factor for which various authors derive different expressions.[9] We take a simple one from Rossi

$$G=2\ln 181Z^{-\frac{1}{3}}.$$

When the protons arrive at the end of their range R_0, which point we take as the origin of x, then the total average increase in path length, representing a correction for the range, is given by

$$\Delta R_{\text{Av}}=\frac{1}{2}\int_{-R_0}^{0}\langle\vartheta^2(x)\rangle_{\text{Av}}dx. \tag{4}$$

The integrals in (3) and (4) can be evaluated numerically, but we can use the crude approximation that $p^2v^2=Cx$, corresponding to the approximate law that the range is proportional to the square of the energy. The result then becomes particularly simple;

$$\Delta R_{\text{Av}}/R_0=4\pi Ne^4Z^2GC^{-1}. \tag{5}$$

The relative correction for the range is independent of the proton energy, and is larger for elements with high Z. The values $\Delta R_{\text{Av}}/R_0$, using Eq. (5), are given in Table V, and the corresponding corrections in the ionization potential have been included in I_{corr} in Table IV. Similar corrections should probably be applied to the ionization potential obtained from experiments at lower energies. If a more correct relation $p^2v^2=Cx^\alpha$, with α between 1.1 and 1.2 is used, then the relative correction would become even more important at lower energies.

TABLE IV. Experimental values for the mass stopping power and mean ionization potential.

Element	Relative mass stopping power at 70 Mev	Energy (Mev)	I_{exp} (ev)	I_{corr} (ev)
Al	1.221	50–75	159	161
		35–50	162	164
Cu	1.000	90–115	355	365
		50–90	365	375
Pb	0.747	70–115	895	970

The correction has not been applied to the experimental range, since the real range will not be observed.

The calculations are valid only when $\langle\vartheta^2\rangle_{\text{Av}}\ll 1$. During the last part of the track this condition is not satisfied. For protons of 100 Mev, however, the energies below 10 Mev contribute only 5 percent to ΔR_{Av}. The influence of this last part of the range can be neglected.

It is more serious that our estimate ignores the correlation between angular deviations at different distances x in each individual proton track. It may turn out that the distribution in ΔR is not normal. More precise calculations should be based on detailed distribution functions given by Fermi, Snyder, and Scott.[10]

The effect of multiple scattering on the straggling is even larger. Obviously, individual tracks will deviate more or less from the straight path. Assuming now that the distribution in ΔR is normal, it seems reasonable to take the root-mean-square deviation equal to $\gamma\Delta R_{\text{Av}}$, where γ is of the order of unity. This causes an additional straggling, which has to be added quadratically to the straggling, caused by fluctuations in the specific ionization along the individual tracks. This latter

[7] R. R. Wilson, Phys. Rev. **60**, 749 (1941).
[8] B. Rossi and K. Greisen, Revs. Modern Phys. **13**, 249 (1941).
[9] Groetzinger, Berger, and Ribe, Phys. Rev. **77**, 584 (1950).
[10] W. T. Scott and H. S. Snyder, Phys. Rev. **78**, 223 (1950).

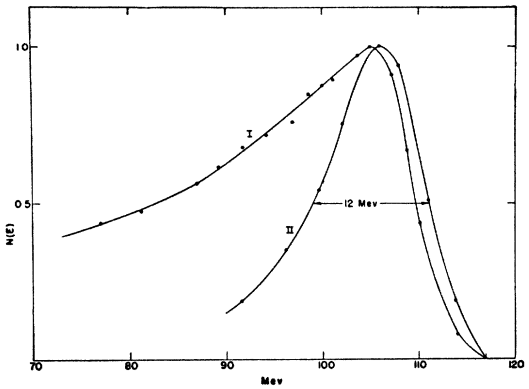

FIG. 6. The distribution of proton energies in the internal beam, hitting a beryllium target $\frac{1}{8}$ in. thick, (curve I) and a tungsten target 0.01 in. thick, (curve II). Both targets were at a 40-in. radius.

effect can be calculated with formulas given by Livingston and Bethe. It is expressed in a straggling parameter s, defined as the difference between the mean and extrapolated range. The corrected straggling is then given by

$$s^2_{\text{corr}}=\tfrac{1}{2}\pi\gamma^2(\Delta R_{\text{Av}})^2+s^2. \tag{6}$$

The values of s and s_{corr} are compared with the experimental values s_{exp} in Table V. We have put $\frac{1}{2}\pi\gamma^2=1$. It is seen that the agreement between theory and experiment becomes very good if the effect of multiple scattering is taken into account. Otherwise, there would be rather large deviations, of 30 percent, outside the experimental error of 10 percent for the heavy element. An important factor in these straggling experiments was that the aperture of the scattered beam is only 0.7°. Therefore, no appreciable increase in straggling can arise from the finite aperture.

IV. THE ENERGY DISTRIBUTION IN THE INTERNAL BEAM

This distribution can be obtained from the same photograph, represented in Fig. 2, as the range. The film is now photometered for various values of r. The maximum density is not the same for all values of r, since the number of protons hitting a unit area of the plate depends on the energy. This number $n(r, y)$ is related to the measured density by Eq. (2). We are interested, however, in $N(E)$, the number of protons per unit energy interval at the scatterer. Let $f(\varphi)d\varphi$ be the vertical angular distribution from the scatterer, for which we can take a gaussian with a mean square deviation $\langle\varphi^2\rangle_{\text{Av}}=\frac{1}{2}\langle\vartheta^2\rangle_{\text{Av}}$ given by Eq. (3). The relationship between the variables φ, E and r, y is given by

$$\begin{aligned}\varphi&=2y/[\pi(r+r_0)],\\ E&=\text{constant}\times(r+r_0)^2,\end{aligned} \tag{7}$$

where r_0 and r are the radial positions of the target and the location in the photographic plate, measured from the center in opposite directions, and y is the distance of the plate from the median plane. The transformation jacobian is readily seen to be a constant. Hence,

$$N(E)f(\varphi)=Kn(r, y), \tag{8}$$

where K is a constant, and $f(\varphi)$ is related to the energy by Eq. (3). But under our experimental conditions $f(\varphi)$ did not vary by more than 10 percent. For thick targets the calculation of $\langle\varphi^2\rangle_{\text{Av}}$ is not reliable, since one does not know the actual path of the protons hitting the edge of the target. In principle, $f(\varphi)$ could be determined experimentally by photometering a photographic film without absorber in the vertical direction.

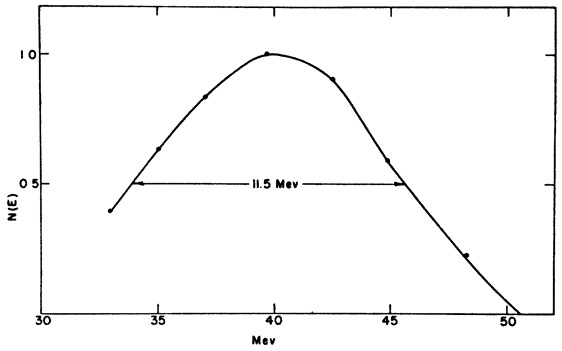

FIG. 7. The distribution of proton energies in the internal beam, hitting a tungsten target (0.01 in. thick) at a 25-in. radius.

In Fig. 6, the distributions $N(E)$ for a beryllium target, $\frac{1}{8}$ in. thick, and a tungsten target, 0.01 in. thick, at a 40-in. radius are given and in Fig. 7 the distribution for the same tungsten target at 25 in. The width of the distribution is about 12 Mev, independent of the radius, and the maximum is about 12 Mev below the maximum energy, corresponding to the equilibrium orbit at the target radius.

Calculations show that multiple traversals with corresponding energy loss cannot explain the distribution for the thin target. A change in the vertical aperture of the cyclotron by clippers did not effect the distribution nor did the use of thinner targets. The broad tail of the distribution of the thick beryllium target, however, must undoubtedly be ascribed to this cause. Light elements with small scattering favor multiple traversals and a corresponding energy spread by ioniza-

TABLE V. The range correction for multiple scattering and the straggling parameter.

Element	Energy (Mev)	$\Delta R_{\text{Av}}/R_0$	s (g/cm²)	s_{corr} (g/cm²)	s_{exp} (g/cm²)
Al	75.8	0.23%	0.084	0.085	0.088
Cu	110.		0.225	0.24	0.25
	72.6	0.53%	0.12	0.125	0.13
Pb	106.6		0.30	0.41	0.37
	95.0	1.5%	0.235	0.32	0.32

tion loss. For reliable results the distribution should be checked in each experiment with the internal beam.[11]

The energy distribution for thin targets represents, probably, a distribution in the amplitudes of radial oscillations which originate near the center of the cyclotron, the average amplitude being 2.5 in. The distribution did not change by more than 20 percent in width under a variation of operating conditions, like tank pressure and firing time of the ion source in the modulation cycle.[12] Rainwater[13] gives three possible reasons for radial oscillation. First, starting the ions off center, and second, azimuthal inhomogeneities in the magnetic field, which could have only a very small effect in our case. There remains the third possibility, that the dc bias field of the dee causes the radial oscillation. An

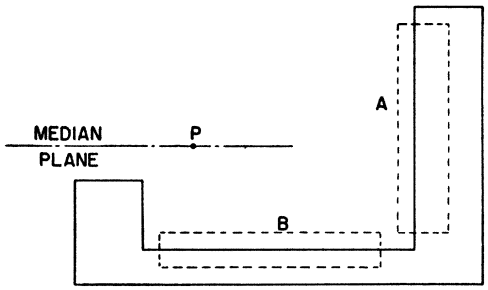

FIG. 8. The targets A and B used to determine the radial oscillations in the beam near the point P, where $n=0.2$.

estimate of this effect gives the right order of magnitude. A change in dee-bias voltage from 2000v to 1000v, however, did not change the distribution by more than 10 percent. According to theory, the width should be proportional to the dee-bias voltage.

Another method of determining the radial oscillations was recently suggested at Harwell,[14] using a C-shaped target as represented in Fig. 8. Only particles with small vertical oscillations will pass the edge.

[11] D. Bodansky and N. F. Ramsey, Phys. Rev. 82, 831 (1951); and Birge, Kruse, and Ramsey, Phys. Rev. 83, 274 (1951).

[12] Under the rather special conditions of an experiment by Birge, Kruse, and Ramsey (see reference 11) a reduction in the width of 35 percent was found.

[13] J. Rainwater, mimeographed notes, "Some factors involved in the theory and operation of an F.M. cyclotron."

[14] M. Snowden, Proceedings of the Harwell Nuclear Physics Conference (1950).

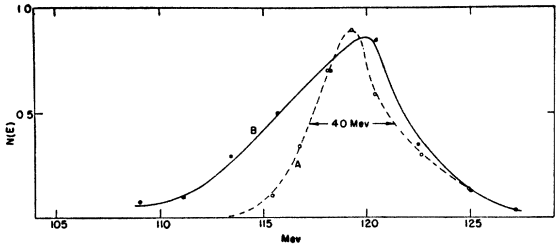

FIG. 9. The distribution of the proton energies at the point P, according to the Harwell method.

The beam then reaches the point P, where the logarithmic gradient of the magnetic field $n=0.2$, and starts blowing up. The blown-up beam will at least partially hit the horizontal target B, but many particles will still hit the vertical target A beyond the point P. It was assumed that the beam will only blow up if the equilibrium orbit reaches the point P. Therefore, target A would be hit by all particles with a radial amplitude larger than the distance AP.

We have applied this method. The carbon activity of the polyethylene target A was measured as a function of the distance PA and differentiated. The activity of sections of target B at different distances from P was also measured. The two distributions which should be approximately the same are represented in Fig. 9. It is seen that the distribution so obtained does not agree with our previous results. The basic assumption that the orbit will blow up when the equilibrium radius is at $n=0.2$ is not justified. By analyzing a particular orbit, it was found that a proton may acquire a considerable, vertical deflection when it spends a couple of revolutions near P, where the gradient in the field is large, even though its equilibrium orbit may be at a radius which is 3 in. smaller. Furthermore, some particles with very small radial amplitudes should not blow up at all and always hit target A. The method can only be applied near the point P and seems to depend critically on the behavior of the magnetic field near the edge of the poles. Therefore, the method of 180° focusing is more reliable.

The authors wish to thank Professor N. F. Ramsey for stimulating discussions and Mr. A. C. Grant and other members of the cyclotron crew for their cooperation during the bombardments.